^{6}Li + ^{15}N interaction at $E_{\text{c.m.}} = 23.1$ MeV: Validation of the $\alpha + d$ cluster model of ^{6}Li

A. T. Rudchik,[1] A. A. Rudchik,[1] O. O. Chepurnov,[1] K. Rusek,[2] N. Keeley,[3,*] K. W. Kemper,[4] S. Kliczewski,[5,†] E. Piasecki,[2] A. Trzcińska,[2] Val. M. Pirnak,[1] O. A. Ponkratenko,[1] I. Strojek,[3] E. I. Koshchy,[6] R. Siudak,[5] S. B. Sakuta,[7] A. P. Ilyin,[1] Yu. M. Stepanenko,[1] Yu. O. Shyrma,[1] V. V. Uleshchenko,[1] K. A. Chercas,[1] H. M. Maridi,[2] and N. Burtebayev[8]

[1]*Institute for Nuclear Research, Ukrainian Academy of Sciences, Prospect Nauki 47, 03680 Kyiv, Ukraine*
[2]*Heavy Ion Laboratory, University of Warsaw, Pasteura 5A, 02-093 Warsaw, Poland*
[3]*National Centre for Nuclear Research, ul. Andrzeja Sołtana 7, 05-400 Otwock, Poland*
[4]*Department of Physics, Florida State University, Tallahassee, Florida 32306, USA*
[5]*H. Niewodniczański Institute of Nuclear Physics, Polish Academy of Sciences, ul. Radzikowskiego 152, 31-342 Kraków, Poland*
[6]*Cyclotron Institute Texas A&M University, College Station, Texas 77843, USA*
[7]*Russian Research Center "Kurchatov Institute", Kurchatov Square 1, 123182 Moscow, Russia*
[8]*Institute of Nuclear Physics, 050032 Almaty, Kazakhstan*

(Received 10 March 2021; accepted 15 April 2021; published 26 April 2021)

An extensive data set for the ^{6}Li + ^{15}N system at an energy $E_{\text{c.m.}} = 23.1$ MeV, consisting of elastic and inelastic scattering to excited states of ^{15}N and the 3^{+}_{1}, 2^{+}_{1}, and 1^{+}_{1} spin-orbit triplet of $L = 2$, $T = 0$ resonances in ^{6}Li, was analyzed with a single calculation including the $^{6}\text{Li} \rightarrow \alpha + d$ breakup, excitation of the ^{15}N levels, and the $^{15}\text{N}(^{6}\text{Li}, ^{7}\text{Li})\,^{14}\text{N}$ one-neutron pickup reaction employing the coupled discretized continuum channel, coupled channel, and coupled reaction channel techniques, respectively. Since the experiment was performed in inverse kinematics, and owing to the specific structure properties of ^{15}N, it was possible to measure an angular distribution for population of the 1^{+}_{1} resonance of ^{6}Li for the first time, without the need for time-consuming and complicated coincidence measurements through detection of the scattered ^{15}N. A good description of the cross sections for populating all three ^{6}Li resonances was obtained, confirming the validity of the $\alpha + d$ cluster model of ^{6}Li. In the methodology adopted the surface absorption was mostly generated by the included couplings, and while the ^{6}Li breakup had the most important influence on the elastic scattering, coupling to the ^{15}N inelastic excitations was also found to have a significant effect, particularly at midrange angles. By contrast, the one-neutron pickup coupling had a negligible effect on the other channels.

DOI: 10.1103/PhysRevC.103.044614

I. INTRODUCTION

Due to its weakly bound nature, combined with a pronounced $\alpha + d$ cluster structure, virtual excitation to the continuum plays an essential role in understanding the elastic scattering of ^{6}Li. This was first demonstrated in connection with the surprising results obtained when the vector analyzing powers for elastic scattering of polarized ^{6,7}Li were measured in the early 1980s; see, e.g., Ref. [1]. In contrast to the predictions of optical model calculations employing folding model spin-orbit potentials, the measured vector analyzing powers for ^{6}Li and ^{7}Li were of opposite sign. It was subsequently shown that this could be explained if the analyzing powers were largely generated by virtual excitation of the projectiles, the static spin-orbit potential making only a weak contribution in both cases [2–5]. The original results were obtained for systems at incident energies close to the Coulomb barrier, but it was later found that the difference in sign of the vector analyzing power for ^{6}Li and ^{7}Li projectiles persisted into the nuclear scattering regime [6].

Fixing the strength of the coupling accurately for ^{6}Li is rendered somewhat more difficult than for ^{7}Li since ^{6}Li has no bound excited states. While it is in principle possible to do so by measuring the $\alpha + d$ coincidences from the decay of the unbound excited states—and this has been done for excitation of the 2.186-MeV 3^{+}_{1} resonance; see e.g., Ref. [7]—such experiments remain difficult, not least due to the large amount of data that has to be collected in order to obtain an adequate number of coincidence events. The collection of sufficient coincidence events to obtain accurate data for excitation of the much more weakly excited members of the ^{6}Li $L = 2$ spin-orbit triplet, the 4.31-MeV 2^{+}_{1} and 5.65-MeV 1^{+}_{1} resonances, would be a formidable task. However, it was found that for systems involving the interaction of ^{6}Li with light targets such as ^{12}C and ^{16}O with high-lying first excited states the ^{6}Li inelastic strength could be measured by scattering a beam of the heavier nucleus from a ^{6}Li target and detecting the inelastically scattered beam particles in the usual way; see, e.g., Ref. [8].

The ^{6}Li + ^{15}N system is in many respects an ideal one for such studies since the first excited state of ^{15}N is the 5.27-MeV $5/2^{+}$, the 2.186-MeV 3^{+}_{1} and 4.31-MeV 2^{+}_{1} levels of ^{6}Li both lying in the gap between this level and the ^{15}N

*Corresponding author: nicholas.keeley@ncbj.gov.pl
†Deceased.

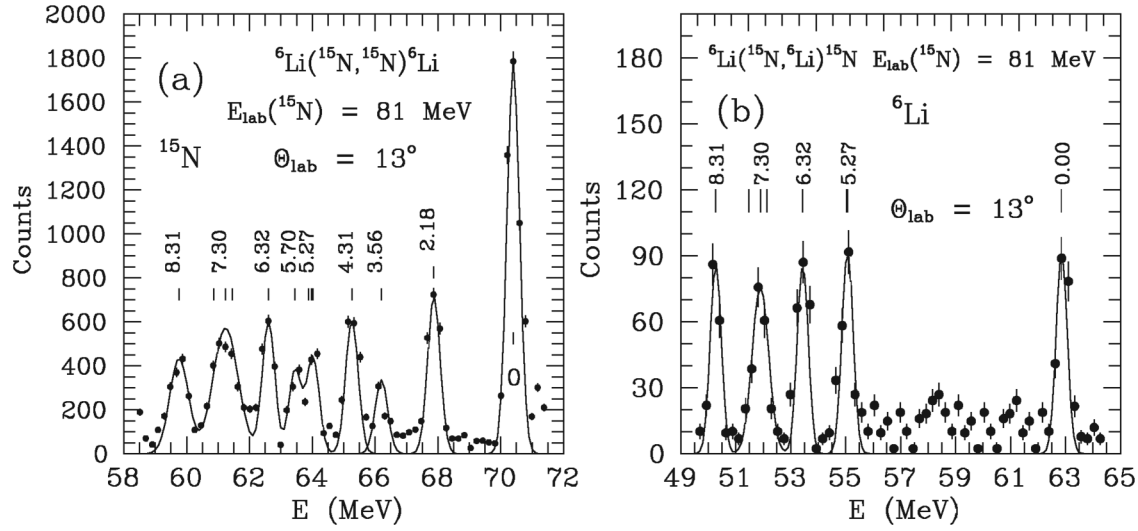

FIG. 1. Typical ^{15}N and ^{6}Li energy spectra from the ^{6}Li(^{15}N, ^{15}N)^{6}Li scattering. The curves denote the fitted symmetric Gaussian forms from which the peak yields were obtained.

ground state, enabling a clean kinematic separation of these levels. In addition, while the 5.65-MeV 1_1^+ level of ^{6}Li is close in excitation energy to the 5.27-MeV $5/2^+$ of ^{15}N the latter is rather weakly excited, enabling the reliable extraction of the ^{6}Li 1_1^+ yield via peak fitting (the 5.30-MeV $1/2^+$ level of ^{15}N is so weakly populated that it may be ignored for all practical purposes). These considerations also mean that inelastic scattering to excited states of both ^{6}Li and ^{15}N may be simultaneously measured with the same detector system. Finally, the extra neutron in ^{15}N outside the ^{14}N core should favor the ^{15}N(^{6}Li, ^{7}Li)^{14}N one-neutron pickup reaction.

High quality data for the ^{6}Li + ^{15}N elastic and inelastic scattering leading to excited states of both projectile and target as well as the one-neutron pickup leading to the ground and first excited states of ^{14}N were recently obtained at the Heavy Ion Laboratory of the University of Warsaw. With modern computers this rich data set may be analyzed with a single calculation incorporating information about the structure of the interacting nuclei as well as the reaction dynamics. These data also provide a stringent test of the ability of the $\alpha + d$ cluster model of ^{6}Li to describe the excitation strengths of all three components of the $L = 2$ spin-orbit triplet, since angular distributions were obtained for excitation of all three levels.

II. EXPERIMENTAL PROCEDURE

Angular distributions for ^{6}Li + ^{15}Nelastic and inelastic scattering were measured using an 81-MeV ^{15}N beam produced by the U-200P cyclotron at the Heavy Ion Laboratory of the University of Warsaw. The beam energy spread on target did not exceed 0.5%. A self-supporting 0.8-mg/cm^2 lithium foil enriched in ^{6}Li to about 85% was used as the target. The experimental beam line and ICARE vacuum chamber containing the target and detector setup detailed in Ref. [9] were used to perform the measurements. The reaction products were detected by four ΔE-E telescopes with 40-μm-thick silicon ΔE detectors and 0.3-mm-thick silicon E detectors. By scattering the heavier ^{15}N ions from the lighter ^{6}Li target nuclei it was possible with these detectors simultaneously to measure the ^{15}N and ^{6}Li particles at forward angles, thus covering both the forward and backward angular ranges for the elastic and inelastic scattering in the center-of-mass system. It was also possible to measure the forward angle cross sections for the unbound excited states in ^{6}Li by extracting their yields from the ^{15}N spectra since the corresponding peaks occur in the 5.3-MeV gap between the ground and first excited states in ^{15}N. A typical ^{6}Li(^{15}N, ^{15}N)^{6}Li spectrum (i.e., detection of the scattered ^{15}N) is shown in Fig. 1(a) where the 2.18-, 3.56-, and 4.31-MeV excited states of ^{6}Li amongst others are clearly observed, while the excitation of the ^{15}N states is seen in the ^{6}Li(^{15}N, ^{6}Li)^{15}N spectrum (i.e., detection of the ^{6}Li recoil) presented in Fig. 1(b).

The solid curves on the spectra of Fig. 1 denote symmetric Gaussian functions fitted to the peaks to extract their yields, which were then used to calculate the differential cross section angular distributions at the angles $\theta_{\text{c.m.}}(^{15}\text{N})$ and $\theta_{\text{c.m.}}(^{15}\text{N}) = 180^\circ - \theta_{\text{c.m.}}(^6\text{Li})$, respectively. In this way, angular distributions for ^{6}Li(^{15}N, ^{15}N)^{6}Li scattering over the whole angular range were determined. The errors in extraction of the peak areas were estimated to be about 20% if the peaks were well resolved and 30–40% for poorly resolved peaks. These errors are greater than the statistical ones. The relative angular distribution of the ^{15}N + ^{6}Li elastic scattering was normalized to calculated optical model (OM) cross sections at small angles, where they are relatively independent of the nuclear potential parameters, by minimizing χ^2 to obtain an overall normalization factor. This factor was then used to convert all the relative angular distribution data into absolute cross sections. The normalization error was smaller than 20%.

III. DATA ANALYSIS

All reaction calculations described in this section were performed with the code FRESCO [10] and all parameter searches were carried out with the SFRESCO package.

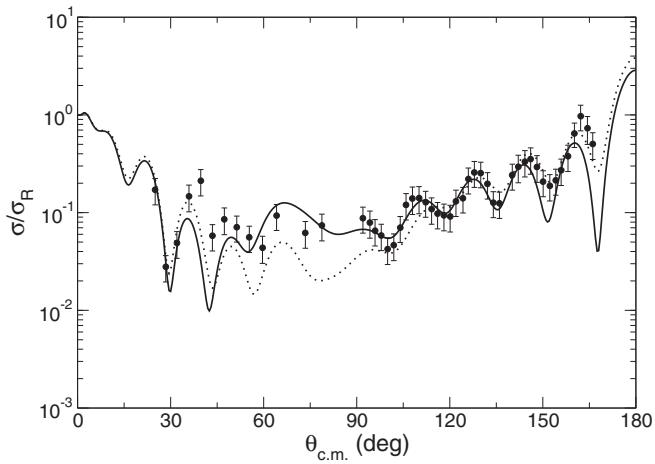

FIG. 2. Comparison of OM (solid curve, $\chi^2 = 1.2$ per data point) and CC (dotted curve, $\chi^2 = 1.4$ per data point) calculations with the elastic scattering data.

A. Coupled channel analysis of the ^{15}N excitations

Before proceeding with large-scale coupled reaction channel (CRC) calculations the influence of the ^{15}N excitations on the elastic scattering was studied using the standard coupled channel (CC) method and a simplified model of the ^{15}N structure. This enabled the nuclear coupling strengths of the most important ^{15}N excitations to be fixed for later use in the complete CRC calculation. As a first step the angular distribution of the elastic scattering differential cross section was fitted with an optical model (OM) calculation using a potential of standard Woods-Saxon (WS) form. The best-fit parameters obtained for the ^{7}Li + ^{15}N system [11] served as the starting point for the search. The result is plotted on Fig. 2 as the solid curve and the parameters of the potential are listed in Table I. The description of the backward angle data is slightly better than at the forward angles, giving an overall value of χ^2 per data point of 1.2. Compared to the ^{7}Li + ^{15}N OM potential obtained at a very similar energy [11] the imaginary part of the ^{6}Li + ^{15}N potential is more diffuse at separations larger than the strong absorption radius, while the real parts are similar. This suggests that the $^6\text{Li} \rightarrow \alpha + d$ breakup, known to be larger in comparison with the $^7\text{Li} \rightarrow \alpha + t$ breakup [12,13], may play a significant role in the ^{6}Li + ^{15}N elastic scattering.

In addition to the elastic scattering, angular distributions for inelastic scattering leading to the (5.270-MeV $5/2^+$ + 5.30-MeV $1/2^+$), 6.323-MeV $3/2^-$, (7.155-MeV $5/2^+$ + 7.301-MeV $3/2^+$ + 7.565-MeV $7/2^+$), and (8.312-MeV $1/2^+$ + 8.571-MeV $3/2^+$) levels of ^{15}N were also obtained. These levels are mostly of single-particle nature (see, e.g., Refs. [14,15]), but for the sake of simplicity they were all treated as collective states. The nuclear coupling potentials were thus implemented as simple derivatives of the diagonal OM potential, scaled by the deformation lengths δ_λ, where λ is the multipolarity of the transition. Only couplings between the ground state and the excited states were considered; no couplings between excited states were included. The ground state and the 6.323-MeV $3/2^-$ state were treated as members of a $K = 1/2$ rotational band, and reorientation of the $3/2^-$ state was included. All the other levels were modeled as if they were vibrational states, i.e., no reorientation couplings were included for these levels.

Information about the strengths of the electromagnetic transitions in ^{15}N is available in the literature [16] and was used to determine the strongest transitions, their multipolarities, and electric matrix elements. Nuclear deformation lengths were obtained by normalizing the calculated angular distributions to the experimental data at forward angles.

The first two excited states of ^{15}N are placed at 5.270 and 5.299 MeV and could not be resolved in the experiment. From the electromagnetic transition studies it follows that the 5.299-MeV state decays to the ground state via an $E1$ transition which is very weak in comparison with the $E3$ transition from the 5.270-MeV state. Therefore, only coupling to the 5.270-MeV $5/2^+$ level was included in the CC calculations. A nuclear deformation length of $\delta_3 = 1.9$ fm was obtained by fitting the calculated curve (dotted curve in Fig. 3) to the data, slightly larger than the value that would be obtained from the measured value of the $B(E3; \text{g.s.} \rightarrow 5/2^+)$ assuming the collective model.

The 6.323-MeV $3/2^-$ level is well separated from the others and, as mentioned above, it was treated as a member of a $K = 1/2$ rotational band. The quadrupole nuclear deformation length obtained from the normalization of the calculated curve (dotted curve in Fig. 3) to the experimental data was $\delta_2 = 1.14$ fm, very close to the value expected from the measured $B(E2; \text{g.s.} \rightarrow 3/2^-)$ value. The CC calculations describe the data reasonably well over the whole angular range, suggesting that the assumption concerning the rotational nature of this state is a reasonable one.

Another group of unresolved excited states is placed at about 7.3 MeV in excitation energy. It consists of three states:

TABLE I. Parameters of the optical model potentials used in the calculations. All radii are defined as $R_i = r_i \times A_T^{1/3}$.

Set	V_0 (MeV)	r_0 (fm)	a_0 (fm)	W_0 (MeV)	r_I (fm)	a_I (fm)	W_d (MeV)	r_d (fm)	a_d (fm)	V_{so} (MeV)	r_{so} (fm)	a_{so} (fm)	Ref.
$\alpha + ^{14}$N	149.8	1.537	0.572	40.0	0.75	0.20							[26]
$d + ^{14}$N	88.19	1.170	0.727	40.0	0.75	0.20				3.51	1.07	0.66	[25]
^{7}Li + ^{14}N	160.0	1.031	0.906				12.75	1.754	0.685				[32]
^{6}Li + ^{14}N	114.2	1.398	0.790				20.3	1.850	0.570				[37]
^{6}Li + ^{15}N	146.0	1.302	0.794	7.91	2.084	1.24							[a]
^{6}Li + ^{15}N	162.8	1.302	0.794	7.16	2.084	1.12							[b]

[a]This work, OM fit.
[b]This work, CC fit.

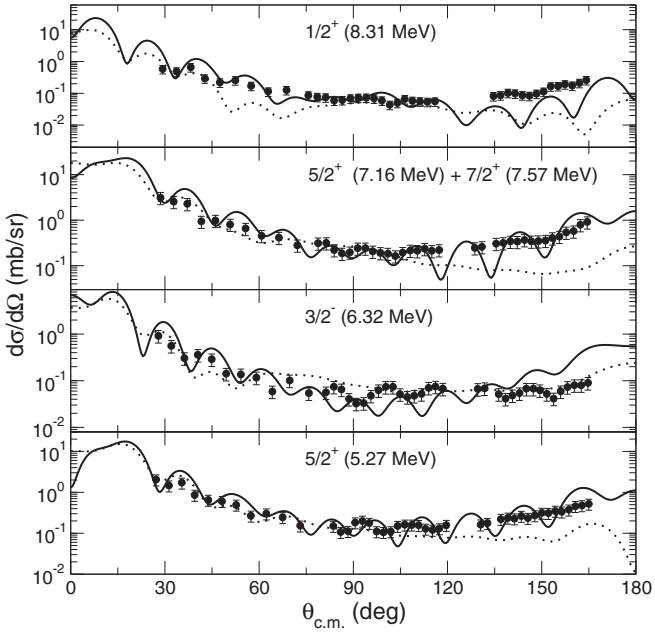

FIG. 3. Results of the CC calculation (dotted curves) compared to the data for inelastic scattering to excited states of ^{15}N. The solid curves denote the results of the final CRC calculation [the results of the CDCC calculations including coupling to the excited states of ^{15}N but not including the ^{15}N(^{6}Li, ^{7}Li)^{14}N one-neutron pickup are graphically indistinguishable].

the 7.155-MeV $5/2^+$, 7.301-MeV $3/2^+$, and 7.565-MeV $7/2^+$. The measured $B(E\lambda;\text{g.s.} \rightarrow \text{exc})$ values indicate that the $E1$ transition to the $3/2^+$ state is weak in comparison with the $E3$ transitions feeding the other two states, so coupling to this state was omitted from the CC calculation. The octupole deformation lengths of the 7.155-MeV $5/2^+$ and 7.565-MeV $7/2^+$ states were kept equal and a value of $\delta_3 = 1.71$ fm was obtained from the fit to the forward angle data (dotted curve in Fig. 3).

The final two unresolved states observed in the experiment were the 8.312-MeV $1/2^+$ and 8.571-MeV $3/2^+$. Both are fed by weak $E1$ transitions so treating them as if they are of collective nature will be very approximate. However, since the goal of this work was to investigate how the target excitations affect the elastic scattering, CC calculations were performed for just one of these levels, the 8.3112-MeV $1/2^+$, with a nuclear deformation length $\delta_1 = 1.50$ fm. This value is much larger than expected from the known dipole reduced transition probability. The CC calculations could describe the data at forward angles only (cf. the dotted curve in Fig. 3).

The effect of coupling to all these inelastic processes on the elastic scattering was found to be rather modest. In order to recover the fit to the elastic scattering data only relatively minor changes in the OM potential were required; see Table I for the parameter values. The elastic scattering angular distribution resulting from the CC calculation including all the inelastic couplings listed above is plotted on Fig. 2 as the dotted curve. The quality of the fit is slightly worse than the OM result, with a χ^2 per data point of 1.4.

B. Cluster structure of ^{6}Li and the role of $^{6}\text{Li} \rightarrow \alpha + d$ breakup

The $\alpha + d$ cluster model of ^{6}Li is among the best structure models for describing the properties of this weakly bound nucleus. In this work the $L = 0$ ground state cluster wave function was calculated assuming a WS binding potential with parameters $R = 1.9$ fm and $a = 0.65$ fm [17]. The three $T = 0$ resonances above the $\alpha + d$ breakup threshold, the 2.186-MeV 3^+, the 4.31-MeV 2^+, and the 5.65-MeV 1^+, were treated as momentum (k) bins, with widths corresponding to 0.1, 2.0, and 3.0 MeV, respectively. Their $L = 2$ cluster wave functions were calculated with WS potentials of the same geometry as for the ground state but with the depths adjusted so that the calculated energies of the resonances were equal to the empirical values. This approach generated reduced transition probabilities between the ground state and the 2.186- and 4.31-MeV resonances of 17.3 and 7.47 $e^2\text{fm}^4$, respectively, close to the measured values [18–20], and 2.65 $e^2\text{fm}^4$ for the transition from the ground state to the 5.65-MeV 1^+ resonance [we are not aware of a measured value of the $B(E2)$ for this transition].

In order to investigate the effect of ^{6}Li breakup on the $^{6}\text{Li} + ^{15}\text{N}$ elastic scattering, the coupled discretized continuum channel (CDCC) method was employed. The continuum of cluster states above the breakup threshold was discretized into momentum bins in a similar way to previous work [21–24]. The continuum was divided into bins of width $\Delta k = 0.2$ fm^{-1}, suitably modified in the presence of the resonant bins described above to avoid double counting, up to a maximum value of $k_{\text{max}} = 1.0$ fm^{-1}, corresponding to a ^{6}Li excitation energy of 17.15 MeV. Relative $\alpha + d$ angular momenta of $L = 0$, 1, 2, and 3 $\hbar$ were included with all allowed couplings, including continuum-continuum couplings, up to multipolarity $\lambda = 4$. The diagonal and all coupling potentials were calculated by Watanabe-type folding of empirical $d + ^{14}$N [25] and $\alpha + ^{14}$N [26] OM potentials obtained at incident energies of about 11 and 22 MeV, respectively (as far as we are aware, similar studies with ^{15}N have not been performed) with the appropriate ^{6}Li $\alpha + d$ cluster wave functions. The imaginary parts of the OM potentials were replaced by a short-ranged potential in order to simulate the incoming-wave boundary condition of Rhoades-Brown and Braun-Munzinger [27]. The parameters are listed in Table I. This model, whereby the majority of the surface absorption is explicitly generated by the various couplings, was adopted in order to test the ability of the basic method (CDCC + CC + CRC calculations) to describe the data without adjustable parameters. The results of CDCC calculations using these potentials are plotted in Figs. 4 and 5 as the dotted curves. Similar results are obtained based on other sets of parameters, for example the $\alpha + ^{14}$N OM potential of England *et al.* [28]. The CDCC calculations reproduce the elastic and inelastic (^{6}Li excitations) scattering results quite well without any adjustable parameters.

C. Role of $^{6}\text{Li}_{\text{g.s.}}$ reorientation

Experiments with polarized ^{6}Li beams have shown that a tensor potential arising from the reorientation of the ^{6}Li ground state plays a remarkable role in the description of

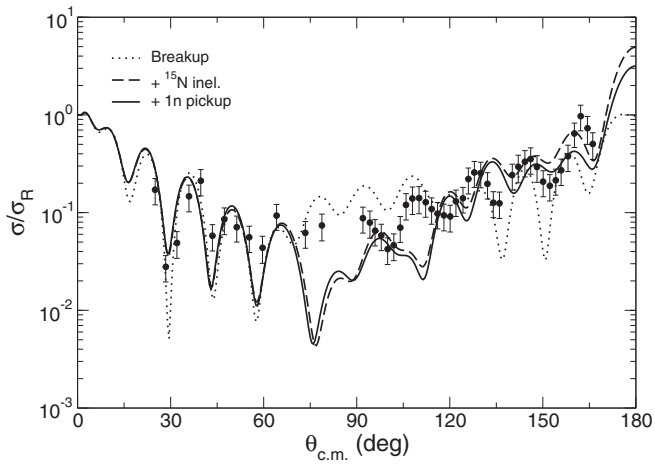

FIG. 4. Angular distribution of the elastic scattering differential cross section (ratio to Rutherford cross section). The dotted curve denotes the result of a CDCC calculation taking the ^{6}Li $\rightarrow \alpha + d$ breakup into account, the dashed curve shows the effect of adding coupling to the inelastic excitations of ^{15}N, and the solid curve shows the result of the final CRC calculation further adding coupling to the ^{15}N(^{6}Li, ^{7}Li) ^{14}N one-neutron pickup reaction.

the experimental analyzing power data by model calculations. Nishioka *et al.* [3] demonstrated that the small negative quadrupole moment of ^{6}Li can be reproduced within the $\alpha + d$ cluster model and is due to cancellation of the large positive quadrupole moment of the deuteron cluster by a negative component generated by the small $L = 2$ admixture in the ^{6}Li ground state wave function. Thus, the ^{6}Li tensor potential is a sum of the two terms: one arising from the D-state admixture

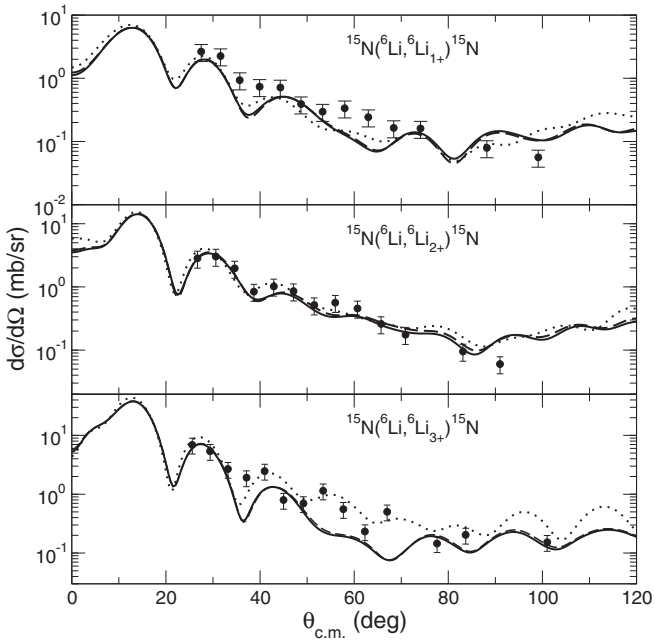

FIG. 5. Angular distributions of the ^{6}Li + ^{15}N inelastic scattering leading to the 2.186-MeV 3^+, 4.31-MeV 2^+, and 5.65-MeV 1^+ resonant states of ^{6}Li. The curves have the same meaning as in Fig. 4.

in the ^{6}Li ground state wave function and the other from the deuteron tensor potential reflecting the deuteron quadrupole moment. To test the influence of the tensor term in the ^{6}Li interaction on the present ^{6}Li + ^{15}N elastic scattering data an effective tensor potential was calculated following the procedure laid down by Nishioka *et al.* [3]. The first term was calculated following Ref. [21] with the spectroscopic amplitude of the $L = 2$ component of the ^{6}Li ground state set to -0.063. The second term was calculated using a deuteron tensor potential adopted from polarized deuteron elastic scattering studies [29].

The cluster model also allows the derivation of a spin-orbit potential for ^{6}Li from the deuteron spin-orbit interaction [3], so such a potential was calculated for the present case using a global deuteron spin-orbit interaction [25]. Both interactions, second-rank tensor and spin-orbit, were added to the CDCC calculations. However, the effect of these interactions on the elastic scattering differential cross section was found to be very small in comparison with that due to the ^{6}Li $\rightarrow \alpha + d$ breakup so they were neglected in the calculations shown here.

D. Coupling to inelastic excitations of ^{15}N

Inelastic excitations of ^{15}N were next added using the nuclear deformation lengths previously determined by the CC calculations presented in Sec. III A. The resulting elastic scattering angular distribution is compared with the data in Fig. 4 (the dashed curve). The influence of these couplings on the elastic scattering angular distribution is significant (the bare optical potential parameters used to calculate the Watanabe folding potentials were not adjusted after including the ^{15}N couplings in this case). They also have a slight influence on the description of the ^{6}Li resonant states; cf. the dashed curves in Fig. 5.

The angular distributions for excitation of the states in ^{15}N are well described, although they are slightly more oscillatory than those produced by the standard CC calculations described in Sec. III A; cf. the solid curves on Fig. 3 (N.B., these curves are actually the result of the final CRC calculation including the one-neutron pickup coupling in addition to the ^{6}Li $\rightarrow \alpha + d$ breakup and ^{15}N inelastic excitations, but the results for the calculations omitting the pickup couplings are indistinguishable on the plot). It is worthy of note that, with the already noted exception of the 6.3-MeV $3/2^-$ state, inclusion of the ^{6}Li $\rightarrow \alpha + d$ breakup couplings leads to a considerable improvement in the description of the backward angle ($\theta_{c.m.} > 90^\circ$) data for inelastic excitation of ^{15}N, introducing a rise in the cross section that matches the data quite well, although the calculated angular distributions tend to be rather more oscillatory than the measured ones.

E. Effect of neutron pickup reactions

In a previous study of the ^{6}Li + ^{18}O system at a similar energy it was found that neutron pickup reactions leading to the low-lying states of ^{17}O made a significant contribution to the backward-angle rise of the elastic scattering differential cross section [23]. In the present case a series of test

calculations was performed with ^{15}N(^{6}Li, ^{7}Li) ^{14}N one-neutron pickup processes included using the CRC method. Transfers leading to the ground (1^+) and 2.31-MeV 0^+, 3.95-MeV 1^+, and 7.03-MeV 2^+ excited states of ^{14}N were included. Spectroscopic amplitudes for the $^{15}\mathrm{N} = {}^{14}\mathrm{N}_{\mathrm{g.s.,exc.}} + n$ overlaps were taken from shell model predictions [30].

The main single-neutron configurations of the ^{7}Li ground state are those involving a nonexcited ^{6}Li core [31]. The $^{7}\mathrm{Li} = {}^{6}\mathrm{Li} + n$ and $^{15}\mathrm{N} = {}^{14}\mathrm{N} + n$ wave functions were calculated using WS binding potentials with the "standard" geometry parameters $r_0 = 1.25$ fm and $a_0 = 0.65$ fm. Two OM potentials [11,32] were tested in the $^{7}\mathrm{Li} + {}^{14}\mathrm{N}$ exit channels, both giving similar results. The effect on the elastic scattering of coupling to the transfer channels was found to be small, much smaller than the inclusion of the ^{15}N inelastic couplings; see Fig. 4. The effect of the pickup couplings on the calculated angular distributions for population of the excited states of ^{15}N and the three $L = 2$ resonances of ^{6}Li was also negligible; see Figs. 3 and 5.

Other transfer processes in addition to the ^{15}N(^{6}Li, ^{7}Li) ^{14}N single-neutron pickup are possible and may have an influence on the elastic scattering. The following reactions were investigated: the ^{15}N(^{6}Li, ^{5}Li) ^{16}N single-neutron stripping, the ^{15}N(^{6}Li, ^{7}Be) ^{14}C single-proton pickup, and the ^{15}N(^{6}Li, ^{5}He) ^{16}O single-proton stripping. The spectroscopic amplitudes S_x of the transferred nucleons and clusters required in the corresponding CRC calculations were calculated within the translationally invariant shell model (TISM) [33] using the code DESNA [34,35] and tables of $1p$-shell wave functions [36]. The influence of coupling to all these transfer reactions was found to be even smaller than that of the single-neutron pickup, therefore they were not considered further in this work.

IV. SUMMARY AND CONCLUSIONS

A new, rather complete, data set for the elastic scattering of ^{6}Li from ^{15}N at a center-of-mass energy of $E_{\mathrm{c.m.}} = 23.1$ MeV was measured in inverse kinematics. The experimental procedure, combined with the particular properties of the excited states of ^{15}N, enabled not only the elastic scattering and inelastic scattering to excited states of ^{15}N to be measured over a wide angular range but also the "inelastic scattering" to the 2.186-MeV 3^+, 4.31-MeV 2^+, and 5.65-MeV 1^+ $L = 2$ resonances of ^{6}Li without the need for complicated and time-consuming coincidence measurements. We believe this is the first time an angular distribution has been measured for the weakly populated 1^+ member of the triplet of $L = 2$, $T = 0$ resonances in ^{6}Li. The whole data set could be described rather well by a single calculation including couplings to the $^{6}\mathrm{Li} \rightarrow \alpha + d$ breakup, inelastic excitations of ^{15}N, and the ^{15}N(^{6}Li, ^{7}Li) ^{14}N single-neutron pickup without adjustable parameters (apart from the nuclear coupling strengths in ^{15}N, which were adjusted to fit the relevant data in a separate CC calculation).

In the model adopted here where the surface absorption is mostly explicitly generated by the couplings, the inelastic excitations of the ^{15}N have a significant influence on the elastic scattering, particularly over the mid-angular range (approximately $\theta_{\mathrm{c.m.}} = 70^\circ$–$105^\circ$) and to a much lesser extent on the angular distributions for "inelastic scattering" leading to the three $L = 2$, $T = 0$ resonances of ^{6}Li. However, the $^{6}\mathrm{Li} \rightarrow \alpha + d$ breakup couplings have by far the most important influence on the elastic scattering. By contrast, coupling to the ^{15}N(^{6}Li, ^{7}Li) ^{14}N one-neutron pickup reaction had a negligible effect on the other channels.

It should be noted that the elastic scattering for angles $\theta_{\mathrm{c.m.}} > 70^\circ$ and, to a lesser extent, the cross section for population of the 5.65-MeV 1^+ resonance of ^{6}Li are sensitive to the details of the continuum binning (Δk, $k_{\max}$, $L_{\max}$, and λ). Extensive tests were carried out and while it was not possible to demonstrate absolute convergence of the continuum model space the result presented here is both numerically stable and physically reasonable. It is also in accord with previous investigations of convergence of the continuum model space for ^{6}Li CDCC calculations; see, e.g., Ref. [38]. The other observables analyzed here, the ^{15}N inelastic cross sections and the cross sections for populating the 2.186-MeV 3^+ and 4.31-MeV 2^+ resonances of ^{6}Li, are much less sensitive to these details and the results presented in Figs. 3 and 5 for these channels are converged.

Bearing this caveat in mind, our conclusions are as follows:

(1) The $\alpha + d$ cluster model of ^{6}Li is confirmed as able to describe well the excitation of all three members of the $L = 0$, $T = 0$ spin-orbit triplet of resonances. Data for population of the 5.65-MeV 1^+ resonance were obtained for the first time and were well described by the cluster model employed within the context of CDCC calculations modeling the $^{6}\mathrm{Li} \rightarrow \alpha + d$ breakup. Tests found that while the details of the calculated cross section for this resonance were sensitive to the details of the continuum model space used, the overall description was not significantly affected. Full convergence of the description of the 2.186-MeV 3^+ and 4.31-MeV 2^+ resonances was, however, demonstrated, so that the simultaneous good description of these two levels provides a stringent test of the model.

(2) Although full convergence of the description of the elastic scattering could not be demonstrated, the cross section for angles $\theta_{\mathrm{c.m.}} > 70^\circ$ being sensitive to the details of the continuum model space, it is possible to conclude that in the model used in this work the couplings to inelastic excitations of ^{15}N have a significant influence on the elastic scattering. This is particularly marked in the mid-angular range, approximately $\theta_{\mathrm{c.m.}} = 70^\circ$–$105^\circ$.

(3) Inclusion of the ^{6}Li breakup couplings in a combined CDCC/CC approach significantly improved the description of the backward angle cross sections for inelastic excitation of ^{15}N compared to the results of standard CC calculations based on a conventional OM potential.

(4) Coupling to the ^{15}N(^{6}Li, ^{7}Li) ^{14}N one-neutron pickup reaction as well as to the other transfer reaction channels was found to have a negligible effect on the other processes included in the final calculation.

The greater sensitivity of the calculated elastic scattering to the choice of continuum model space than is usually observed in calculations of this type possibly reflects an influence of the breakup coupling on the nearside/farside interference effects typical of elastic scattering in the Fraunhofer diffraction regime. Nevertheless, it has been possible satisfactorily to describe a wide body of data with a single calculation involving minimal parameter adjustments. It has also been confirmed that the $\alpha + d$ cluster model, when used in conjunction with the CDCC technique, is able to provide a good description of all three members of the $L = 2$, $T = 0$ spin-orbit triplet of resonances in ^{6}Li.

ACKNOWLEDGMENT

This work was funded in part by the Polish National Agency for Academic Exchange (NAWA) within the Ulam Programme under Grant Agreement No. PPN/ULM/2019/1/00189/U/00001.

[1] G. Tungate, R. Bottger, P. Egelhof, K.-H. Mobius, Z. Moroz, E. Steffens, W. Dreves, I. Koenig, and D. Fick, Phys. Lett. B **98**, 347 (1981).
[2] H. Nishioka, R. C. Johnson, J. A. Tostevin, and K.-I. Kubo, Phys. Rev. Lett. **48**, 1795 (1982).
[3] H. Nishioka, J. A. Tostevin, R. C. Johnson, and K.-I. Kubo, Nucl. Phys. A **415**, 230 (1984).
[4] H. Ohnishi, M. Tanifuji, M. Kamimura, Y. Sakuragi, and M. Yahiro, Nucl. Phys. A **415**, 271 (1984).
[5] F. Petrovich, R. J. Philpott, A. W. Carpenter, and J. A. Carr, Nucl. Phys. A **425**, 609 (1984).
[6] O. A. Momotyuk, N. Keeley, K. W. Kemper, B. T. Roeder, A. M. Crisp, W. Cluff, B. G. Schmidt, M. Wiedeking, F. Maréchal, K. Rusek, S. Yu. Mezhevych, and J. Liendo, Phys. Lett. B **640**, 13 (2006).
[7] H. Gemmeke, B. Deluigi, L. Lassen, and D. Scholz, Z. Phys. A **286**, 73 (1978).
[8] M. F. Vineyard, J. Cook, and K. W. Kemper, Phys. Rev. C **31**, 879 (1985).
[9] A. T. Rudchik, O. V. Herashchenko, K. W. Kemper, K. Rusek, S. Kliczewski, K. A. Chercas, A. A. Rudchik, E. I. Koshchy, V. M. Pirnak, E. Piasecki, A. Trczińska, S. B. Sakuta, R. Siudak, I. Strojek, A. Stolarz, A. O. Barabash, A. P. Ilyin, O. A. Ponkratenko, Yu. M. Stepanenko, Yu. O. Shyrma *et al.*, Nucl. Phys. A **939**, 1 (2015).
[10] I. J. Thompson, Comput. Phys. Rep. **7**, 167 (1988).
[11] A. T. Rudchik, A. A. Rudchik, L. M. Muravynets, K. W. Kemper, K. Rusek, E. Piasecki, A. Trzcińska, E. I. Koshchy, V. M. Pirnak, O. A. Ponkratenko, I. Strojek, A. Stolarz, O. V. Herashchenko, Yu. M. Stepanenko, V. A. Plujko, S. B. Sakuta, R. Siudak, and A. Szczurek, Nucl. Phys. A **958**, 234 (2017).
[12] G. R. Kelly, N. J. Davis, R. P. Ward, B. R. Fulton, G. Tungate, N. Keeley, K. Rusek, E. E. Bartosz, P. D. Cathers, D. D. Caussyn, T. L. Drummer, and K. W. Kemper, Phys. Rev. C **63**, 024601 (2000).
[13] C. Signorini, A. Edifizi, M. Mazzocco, M. Lunardon, D. Fabris, A. Vitturi, P. Scopel, F. Soramel, L. Stroe, G. Prete, E. Fioretto, M. Cinausero, M. Trotta, A. Brondi, R. Moro, G. La Rana, E. Vardaci, A. Ordine, G. Inglima, M. La Commara, D. Pierroutsakou, M. Romoli *et al.*, Phys. Rev. C **67**, 044607 (2003).
[14] G. C. Ball and J. Cerny, Phys. Rev. **177**, 1466 (1969).
[15] C. E. Mertin, D. D. Caussyn, A. M. Crisp, N. Keeley, K. W. Kemper, O. Momotyuk, B. T. Roeder, and A. Volya, Phys. Rev. C **91**, 044317 (2015).
[16] F. Ajzenberg-Selove, Nucl. Phys. A **523**, 1 (1991).
[17] K.-I. Kubo and M. Hirata, Nucl. Phys. A **187**, 186 (1972).
[18] F. Eigenbrod, Z. Phys. **228**, 337 (1969).
[19] M. Bernheim and G. R. Bishop, Phys. Lett. **5**, 270 (1963).
[20] R. Yen, L. S. Cardman, D. Kalinsky, J. R. Legg, and C. K. Bockelman, Nucl. Phys. A **235**, 135 (1974).
[21] K. Rusek, P. V. Green, P. L. Kerr, and K. W. Kemper, Phys. Rev. C **56**, 1895 (1997).
[22] K. Rusek, N. Alamanos, N. Keeley, V. Lapoux, and A. Pakou, Phys. Rev. C **70**, 014603 (2004).
[23] K. Rusek, N. Keeley, K. W. Kemper, and A. T. Rudchik, Phys. Rev. C **91**, 044612 (2015).
[24] A. Pakou, N. Alamanos, N. M. Clarke, N. J. Davis, G. Doukelis, G. Kalyva, M. Kokkoris, A. Lagoyannis, T. J. Mertzimekis, A. Musumarra, N. G. Nicolis, C. Papachristodoulou, N. Patronis, G. Perdikakis, D. Pierroutsakou, D. Roubos, K. Rusek, S. Spyrou, and Ch. Zarkadas, Phys. Lett. B **633**, 691 (2006).
[25] W. W. Daehnick, J. D. Childs, and Z. Vrcelj, Phys. Rev. C **21**, 2253 (1980).
[26] B. T. Lucas, D. R. Ober, and O. E. Johnson, Phys. Rev. **167**, 990 (1967).
[27] M. J. Rhoades-Brown and P. Braun-Munzinger, Phys. Lett. B **136**, 19 (1984).
[28] J. B. A. England, E. Casal, A. Garcia, T. Picazo, J. Aguilar, and H. M. Sen Gupta, Nucl. Phys. A **284**, 29 (1977).
[29] R. Frick, H. Clement, G. Graw, P. Schiemenz, N. Seichert, and Sun Tsu-Hsun, Z. Phys. A **319**, 133 (1984).
[30] S. B. Sakuta, Yu. A. Glukhov, A. T. Rudchik, V. M. Pirnak, A. Budzanowski, S. Kliczewski, R. Siudak, I. Skwirczyńska, and A. Szczurek, Nucl. Phys. A **639**, 599 (1998).
[31] S. Cohen and D. Kurath, Nucl. Phys. A **101**, 1 (1967).
[32] M. E. Cobern, D. J. Pisano, and P. D. Parker, Phys. Rev. C **14**, 491 (1976).
[33] Yu. F. Smirnov and Yu. M. Tchuvil'sky, Phys. Rev. C **15**, 84 (1977).
[34] A. T. Rudchik and Yu. M. Tchuvil'sky. The code DESNA, Report No. KIYAI-82-12, Institute for Nuclear Research, Kiev, 1982 (unpublished).
[35] A. T. Rudchik and Yu. M. Tchuvil'sky, Ukr. Fiz. Zh. **30**, 819 (1985).
[36] A. N. Boyarkina, Structure of 1p-Shell Nuclei, Thesis, Moscow State University, 1973 (unpublished).
[37] K. O. Groeneveld, A. Richter, U. Strohbusch, and B. Zeidman, Phys. Rev. Lett. **27**, 1806 (1971).
[38] Y. Sakuragi, M. Yahiro, and M. Kamimura, Prog. Theor. Phys. Suppl. **89**, 136 (1986).